Published in final edited form as:
Cancer Res. 2010 December 15; 70(24): 10161–10169. doi:10.1158/0008-5472.CAN-10-1921.

The inflammasome component Nlrp3 impairs antitumor vaccine by enhancing the accumulation of tumor-associated myeloid-derived suppressor cells

Hendrik W. van Deventer[1,a], **Joseph E. Burgents**[2,a], **Qing Ping Wu**[3], **Rita-Marie T. Woodford**[4], **W. June Brickey**[2,3], **Irving C. Allen**[2], **Erin McElvania-Tekippe**[2], **Jonathan S. Serody**[1,2,3,b], and **Jenny P-Y Ting**[2,3,4,b]

[1] Department of Medicine, University of North Carolina at Chapel Hill, Chapel Hill, North Carolina, 27599

[2] Department of Microbiology and Immunology, University of North Carolina at Chapel Hill, Chapel Hill, North Carolina, 27599

[3] Lineberger Comprehensive Cancer Center, University of North Carolina at Chapel Hill, Chapel Hill, North Carolina, 27599

[4] School of Dentistry, Oral Biology Program, University of North Carolina at Chapel Hill, Chapel Hill, North Carolina, 27599

Abstract

The inflammasome is a proteolysis complex that generates the active forms of the pro-inflammatory cytokines IL-1β and IL-18. Inflammasome activtation is mediated by NLR proteins that respond to microbial and nonmicrobial stimuli. Among NLRs, NLRP3 senses the widest array of stimuli and enhances adaptive immunity. However, its role in antitumor immunity is unknown. Therefore, we evaluated the function of the NLRP3 inflammasome in the immune response using dendritic cell vaccination against the poorly immunogenic melanoma cell line B16-F10. Vaccination of $Nlrp3^{-/-}$ mice led to a relative 4-fold improvement in survival relative to control animals. Immunity depended upon $CD8^+$ T cells and exhibited immune specificity and memory. Increased vaccine efficacy in $Nlrp3^{-/-}$ hosts did not reflect differences in dendritic cells but rather differences in myeloid-derived suppressor cells (MDSCs). Although Nlrp3 was expressed in MDSCs, the absence of Nlrp3 did not alter either their functional capacity to inhibit T cells or their presence in peripheral lymphoid tissues. Instead, the absence of Nlrp3 caused a 5-fold reduction in the number of tumor-associated MDSCs found in host mice. Adoptive transfer experiments also showed that $Nlrp3^{-/-}$ MDSCs were less efficient in reaching the tumor site. Depleting MDSCs with an anti-Gr-1 antibody increased the survival of tumor-bearing wild-type mice but not $Nlrp3^{-/-}$ mice. We concluded that Nlrp3 was critical for accumulation of MDSCs in tumors and for inhibition of antitumor T cell immunity after dendritic cell vaccination. Our findings establish an unexpected role for Nlrp3 in impeding antitumor immune responses, suggesting novel approaches to improve the response to antitumor vaccines by limiting Nlrp3 signaling.

Keywords

Nlrp3; inflammasome; cancer vaccine; myeloid-derived suppressor cell

Corresponding Author: Jonathan S. Serody, 450 West Drive, Lineberger Comprehensive Cancer Center, CB#7295, Chapel Hill, NC 27599-7295 Telephone: (919) 966-8644. Fax: (919) 966-8212. serody@med.unc.edu.
[a,b]These authors have contributed equally to this work.

Introduction

NLR family, pyrin domain containing 3 (Nlrp3) is a member of the nucleotide-binding domain and leucine-rich repeat containing gene family of intracellular sensors. When activated, Nlrp3 forms a protein complex called the inflammasome (1–3). The inflammasome combines Nlrp3 with the adaptor molecule ASC/PYCARD/TMS/CARD5, Cardinal, and pro-caspase-1 (4) to form a multimer. The result is the proteolytic maturation of caspase-1, which cleaves and activates proIL-1β and proIL-18 to generate IL-1β and IL-18 (3).

Nlrp3 senses a variety of microbial and nonmicrobial molecular motifs. The microbial signals are part of the pathogen associated molecular patterns or PAMPs and include gram positive and negative bacteria, RNA and DNA viruses, polyinosinic:polycytidylic acid, and LPS (1). The nonmicrobial signals include exogenous compounds such as asbestos and endogenous signals such as urate crystals (1). Many of these nonmicrobial stimuli are referred to as damage associated molecular patterns or DAMPs (5). Activation by these signals not only promotes innate immunity but also enhances Th1, Th2 and Th17 responses (6). Thus, the inflammasome responds to many pathological insults and participates in multiple immune pathways (7).

In contrast to this literature on PAMPs and DAMPs, there have been few studies characterizing Nlrp3 in the tumor microenvironment though stimuli for its activation are no doubt present (8). However, studies on Il-1β suggest a potential tumor promoting role in several mouse models (9–10). Conversely, reduction of IL-1β diminished metastases to the lung (11) and eliminating IL-1β prevented progression in a murine melanoma model (12).

Human studies have been less definitive but remain consistent with the murine data. For example, gastric cancer is associated with genetic polymorphisms linked to enhanced IL-1β expression (13). Similar studies on IL-18 polymorphisms have demonstrated an increased risk for other epithelial cancers (14). More directly, serum IL-18 concentrations are inversely correlated with survival in hepatocellular cancer (15).

These cytokines can contribute to tumorigenesis in several ways though more recent attention has focused on their role in promoting myeloid-derived suppressor cells (MDSCs) (16–17). MDSCs are a heterogeneous population of immature myeloid cells that are most readily identified in the mouse by their expression of Gr-1 and CD11b (18). These cells suppress T cell responses directly by a variety of mechanisms (19). MDSCs also contribute to tumorigenesis indirectly by inducing regulatory T cells (20) and a Th2 immune response (21), suppressing NK cells (22), and increasing angiogenesis (23). Clinical studies have documented these cells in several human cancers (24) including head and neck (25), renal cell (26), and hepatocellular (22) cancers. Both murine and human studies have found the number of MDSCs increases with tumor burden (24,27).

These data suggest Nlrp3 activation could inhibit the antitumor immune response to a cancer vaccine by enhancing the function of immunosuppressive cells. We were led to test this hypothesis after completing gene array studies that showed an association between Nlrp3 and MDSCs.

Materials and Methods

Mice

Nlrp3$^{-/-}$ mice were generated as described (28). *EGFP* X *Nlrp3*$^{-/-}$ transgenic mice were produced by crossing F1 progeny of *EGFP* transgenic and homozygous *Nlrp3*$^{-/-}$ mice. All other mice were purchased from Jackson Laboratories. All experiments were conducted using protocols approved by Institutional Animal Care and Use Committee of the University of North Carolina at Chapel Hill.

Dendritic Cell Vaccination Model

Tumor lines were purchased from the American Type Culture Collection and were expanded by six passages in 7.5% FCS/DMEM (Gibco). B16-F10 cells were authenticated by the presence of melanin. Subcutaneous tumors were formed by injecting either 1×10^4 cells (B16-F10, Lewis Lung) or 5×10^5 cells (E.G7-OVA) in the left leg. The leg diameter was measured three times a week. Mice were euthanized when this diameter was > 6 mm and the survival time was interpolated from the last two measurements. A tumor was designated as "non-palpable" if the left leg diameter was within 0.2mm of the right leg *and* the tumor was visible on gross dissection.

DCs were generated from bone marrow cultures treated with GM-CSF and IL-4 (Peprotech Inc) (29). DCs were pulsed at an 8:1 ratio with B16-F10 lysates formed by irradiation (16,000 rads), five rounds of freeze/thaw, and shearing by a 30 gauge needle. After antigen pulsing, DCs were matured with 100 ng/ml of LPS for 24 hours. 1×10^6 cells were subcutaneously injected on day three and ten after tumor injection.

Cell depletion was accomplished by the intraperitoneal injection of 200 mcg of PK136 (NK cell) and RB6-8C5 (MDSC) and 500 mcg of 53.6.72 (CD8 T cell) and GK1.5 (CD4 T cell) mAb (BioExpress). The injection schedule for lymphoid cell depletion was day -1, day 0 and then biweekly. MDSC depletion injections were biweekly starting on day 6.

Flow Cytometry

Flow cytometry was performed as previously described (30). For the migration assays, MDSCs were harvested from the spleens of EGFP transgenic C57BL/6 or *Nlrp3*$^{-/-}$ mice by immunomagnetic bead separation (Miltenyi) two weeks after intravenous tumor injection. These cells were then cryopreserved. *Nlrp3*$^{-/-}$ mice were injected with 25,000 B16-F10 cells while WT received 1×10^4. When the tumor was palpable, the mice received an intravenous injection of 5×10^5 EGFP MDSCs. Three days after this injection, the tumor was harvested, digested, and processed flow cytometry.

MDSC Assay

MDSCs for the in vitro suppression assays were harvested by FACS sorting from the lungs of WT and *Nlrp3*$^{-/-}$ mice two weeks after intravenous injection with 1×10^6 B16-F10 cells. Immunosuppression was evaluated by adding these cells to a MLR. Stimulator cells were taken from the adherent fraction of BALB/cJ splenocytes after two hours of culture; responder cells were harvested from the non-adherent fraction of C57BL/6J splenocytes. Stimulators and CD11b$^+$ Gr-1$^+$ cells were treated with mitomycin C and responders were labeled with CFSE.

Real time PCR

Total RNA was isolated from sorted cells using RNeasy columns (Qiagen) and converted to cDNA with random hexamers and MMLV Reverse Transcriptase (Invitrogen). PCR

amplification was performed using *Nlrp3* specific primers and probe: 5′-CTCCCGCATCTCCATTTGT-3′, 5′-GCGTGTAGCGACTGTTGA-3′, and FAM-CCACACTCTCACCTAGACGCGC-TAMRA with TaqMan PCR reagents and 7900HT Thermocycler (Applied Biosystems). Expression values were normalized to cell number.

Statistics

Data are reported as a mean ± standard error of the mean (SEM). Results were considered significant if $p \leq 0.05$ as determined by the Mann Whitney test. Comparisons in survival were done by the Cox proportional hazard regression method

Results

The Nlrp3 is expressed in myeloid derived suppressor cells (MDSCs)

We have previously shown peripheral tolerance mechanisms are a major impediment to successful anti-tumor vaccines in the FVB/neu mouse (31). In order to delineate mechanisms by which MDSCs function in this model, we utilized Affymetrix whole mouse genome arrays to compare gene expression from Gr-1$^+$, CD11b$^+$ MDSCs isolated from the spleen with those from the tumor. This experiment revealed that 16 genes were upregulated by more than threefold in the tumor-associated MDSCs (Supplementary Table S1). Of these 16 genes, *Nlrp3* and *Il-1β* were substantially increased in expression (*Nlrp3* 11.9 ± 3.2 fold; *Il-1β* 3.85 ± 0.7 fold) in the tumor environment. These results suggested activation of the Nlrp3 inflammasome occurs in MDSCs present in the tumor microenvironment.

We tested the role of the Nlrp3 inflammasome more directly using the B16-F10 tumor and B6 mice whose background would allow us to compare wild type (WT) with *Nlrp3*$^{-/-}$ mice. First, we verified the expression of *Nlrp3* in the tumor-associated Gr-1$^+$, CD11b$^+$ cells, which had been isolated by cell sorting. Both Gr-1$^+$, CD11b$^+$ and Gr-1$^-$, CD11b$^+$ cells expressed *Nlrp3* at transcript numbers significantly greater than found in CD11b$^-$ cells (*4.30 ± 0.13, 4.69 ± 0.94 vs. 0.00 ± 0.0, p = 0.033*) (Fig. 1A). *Nlrp3* was not expressed in *Nlrp3*$^{-/-}$ mice (Fig. 1B).

Dendritic cell vaccination improves survival in *Nlrp3*$^{-/-}$ mice

We then compared the survival of WT and *Nlrp3*$^{-/-}$ mice that received a subcutaneous injection of 1×10^4 B16-F10 melanoma cells. In this model, none of the WT or *Nlrp3*$^{-/-}$ mice survived (Fig. 2A). The median survival was also not significantly different (15.3 vs. 16.6 days, *p = NS*).

The survival of *Nlrp3*$^{-/-}$ mice could be improved by administering a DC vaccine on days 3 and 10 *after* tumor injection. In these experiments, mice received inoculations of 1×10^6 WT DCs pulsed with B16-F10 tumor cell lysate. Although only 9.1% of the WT mice demonstrated long term survival, survival in the *Nlrp3*$^{-/-}$ mice increased to 35%. The hazard ratio favoring survival in the *Nlrp3*$^{-/-}$ mice was 2.4 (1.2 – 4.8) (*p = 0.017*) (Fig. 2B).

The survival benefit was not limited to the B16-F10 model. WT and *Nlrp3*$^{-/-}$ mice were also subcutaneously injected with 5×10^5 E.G7-OVA tumor cells and then treated with peptide pulsed DCs using the same schedule. As before, *Nlrp3*$^{-/-}$ mice had a substantial improvement in survival compared to WT mice (33.3% vs. 62.5%). The hazard ratio favoring survival in the *Nlrp3*$^{-/-}$ mice was 2.1 (1.6 – 3.1) (*p = 0.023*) (Supplementary Fig. S1).

Nlrp3 expression by the host limits the effectiveness of the DC vaccine

Since this survival advantage may have been dependent on the expression of Nlrp3 by the DCs, we compared survival in *Nlrp3*$^{-/-}$ mice treated with DC vaccines from WT or *Nlrp3*$^{-/-}$ mice. Thirty three percent of the *Nlrp3*$^{-/-}$ mice injected with *Nlrp3*$^{-/-}$ DC vaccine survived compared to 40% injected with the WT vaccine (*p = NS*) (Fig. 2C). Thus, the *Nlrp3*$^{-/-}$ DC vaccine produced survival that was comparable to WT vaccines in *Nlrp3*$^{-/-}$ mice.

Subsequently, we evaluated the effectiveness of vaccination using *Nlrp3*$^{-/-}$ and WT DCs in WT mice. None of the WT mice survived. Those receiving the WT vaccine had a median survival of 21.8 days versus 16.1 days with the *Nlrp3*$^{-/-}$ vaccine (*p=NS*) (Fig. 2D). From these data, we concluded the poor outcome in WT mice was due to Nlrp3 expression by host cells and not by the cells given with the vaccine.

The benefit of the DC vaccine in *Nlrp3*$^{-/-}$ mice is CD8 dependent

The immunologic memory of the vaccinated *Nlrp3*$^{-/-}$ mice was tested by rechallenging these mice three months after their initial tumor exposure. Ten of the eleven rechallenged *Nlrp3*$^{-/-}$ mice survived a second tumor injection (90.9%) (Fig. 3A). Two of the surviving WT mice were also rechallenged and one survived (50%). Due to the low number of surviving WT mice, we were unable to establish statistical significance. Nevertheless, these experiments demonstrated an antitumor memory response in the *Nlrp3*$^{-/-}$ mice and implied the improved outcome was due to an enhanced immune response to the vaccine.

The specificity of this tumor protection was examined by challenging surviving *Nlrp3*$^{-/-}$ mice with an unrelated tumor. Eight *Nlrp3*$^{-/-}$ mice received 1×10^4 Lewis lung carcinoma cells (LLCa) and two mice survived (25%) (Fig. 3A). This result was significantly less than those rechallenged with B16-F10 cells (*p = 0.003*) but not different from naive *Nlrp3*$^{-/-}$ mice injected LLCa cells (*survival = 20%*). Therefore, the immunological memory generated after vaccination in *Nlrp3*$^{-/-}$ mice was specific only for the tumor used in the vaccine.

The efficacy of the adaptive immune response was further tested by measuring survival after antibody depletion of $CD4^+$, $CD8^+$, or NK cells (Supplementary Fig. S2). The effect of cell depletion was measured by calculating a hazard ratio using Cox regression analysis. The survival of all three cohorts of cell-depleted *Nlrp3*$^{-/-}$ mice was decreased compared to the control *Nlrp3*$^{-/-}$ mice (Fig. 3B, C). However, this finding was only statistically significant for *Nlrp3*$^{-/-}$ mice after the depletion of $CD8^+$ T cells (*HR = 2.06, p = 0.028*). Therefore, the enhanced activity of tumor vaccination in the *Nlrp3* $^{-/-}$ mice required $CD8^+$ T cells.

This conclusion was supported by determining the number of CD8 effector T cells from the lymph nodes of DC vaccinated mice. Tumor-draining nodes were harvested on day 14 following DC vaccinations on day 3 and 10. The number of $CD62L^{lo}$, $CD69^{hi}$ effector cells was measured by flow cytometry. There were no differences in the number of CD8 effector cells between WT and *Nlrp3*$^{-/-}$ mice either with or without tumor injection. However, differences became apparent when the tumor injected mice were further subdivided into groups with palpable or non-palpable tumors. Using this analysis, *Nlrp3*$^{-/-}$ mice with no palpable tumor had significantly more CD8 effector cells than WT mice (18.1 ± 0.4 *vs*.$3.5 \pm 0.5 \times10^4$ cells, *p = 0.002*) (Fig. 3D). There were no differences in the number of CD4 effectors or in the number of $CD8^+$ cells in mice with palpable tumors.

Nlrp3$^{-/-}$ MDSCs are morphologically and functionally equivalent to WT MDSCs in vitro

Given this result, we compared the microscopic appearance and the functional activity of MDSCs from *Nlrp3*$^{-/-}$ and WT tumor-bearing mice. Tumor-associated MDSCs from both mice could be further divided into two subpopulations based on their expression of Gr-1 and CD11b. The Gr-1^{Hi}, CD11b^{+} cells had a neutrophil morphology and the Gr-1^{Int}, CD11b^{+} cells had a monocytic morphology. These subpopulations corresponded to the granulocytic and monocytic MDSCs described by Youn et al. (32). However, there were no microscopic differences between *Nlrp3*$^{-/-}$ or WT MDSCs within each subpopulation (Fig. 4A).

Since the numbers of MDSCs within the tumors were inadequate for *in vitro* suppression assays, we isolated these cells from the lungs of WT and *Nlrp3*$^{-/-}$ mice with B16-F10 metastasis. Once again, two subpopulations of MDSCs could be identified by CD11b and Gr-1 expression. The monocytic MDSCs displayed a greater suppressive capacity compared to the granulocytic MDSCs. However, we did not find differences in T cell suppression between WT and *Nlrp3*$^{-/-}$ MDSCs from either subpopulation (Fig. 4B). There were also no differences in the suppressive ability of MDSCs isolated from the spleens of WT and *Nlrp3*$^{-/-}$ mice with metastatic melanoma after DC vaccination (Supplementary Fig. S3).

Regardless of the differences among Gr-1^{Hi} and Gr-1^{Int} MDSCs, the central observation from these experiments was no differences were detected when comparing cells from WT and *Nlrp3*$^{-/-}$ mice. These data indicate the disparity in the vaccine response between the WT and *Nlrp3*$^{-/-}$ mice was not due to differences in the suppressive capacity of their respective MDSCs.

Nlrp3$^{-/-}$ mice have fewer MDSCs at the tumor site

Since the survival advantage of the *Nlrp3*$^{-/-}$ mouse could not be explained by functional differences in MDSCs, we hypothesized this advantage was due to a reduction in the number of MDSCs. We found no significant differences in the number of Gr-1^{+}, CD11b^{+} cells isolated from tumor draining lymph node (TDLN) 14 days after tumor injection (Fig 5A). There was a trend to a lower percentage of splenic MDSCs in the *Nlrp3*$^{-/-}$ mice but this finding was not statistically significant (*1.61 ± 0.24% vs. 2.67 ± 0.40%, p = 0.11*) (Fig. 5A).

We next evaluated the number of MDSCs within the tumor by immunofluorescent microscopy. Mice were included in this analysis if their tumor was visible by light microscopy. This approach revealed a five fold increase in the number of CD11b/Gr-1^{+} cells in the tumor and surrounding stroma of WT mice compared to *Nlrp3*$^{-/-}$ mice (*18.6 ± 3.0/LPF vs. 3.5 ± 0.5/LPF, p = 0.02*) (Fig. 5B, Supplementary Fig. S4).

Since immunohistochemistry cannot distinguish between Gr-1^{Hi} and Gr-1^{Int} cells, the percentage of these two populations was measured using flow cytometry. Tumors were harvested when palpable; mice without tumor were excluded. Gating on the Gr-1^{Int}, CD11b^{+} cells revealed a 4.7 fold increase of the monocytic MDSCs in WT mice compared to *Nlrp3*$^{-/-}$ mice (*2.1 ± 0.5% vs. 0.45 ± 0.24%, p = 0.003*), while a six fold increase was noted in the granulocytic MDSCs (*0.54 ± 0.18% vs. 0.09%, p = 0.003*) (Fig. 5C). Thus, both flow cytometry and immunohistochemistry demonstrated a significant reduction in the number of tumor-associated MDSCs in *Nlrp3*$^{-/-}$ compared to WT mice.

Depletion of MDSCs improves survival in vaccinated WT but not *Nlrp3*$^{-/-}$ mice

We established that the decrease in MDSCs accounted for the improved survival in *Nlrp3*$^{-/-}$ mice by measuring survival following MDSC depletion. Anti-Gr-1 antibody was injected twice a week beginning on day six. This treatment produced a 2.6 fold decrease in MDSCs (Supplementary Fig. S5). Depletion of MDSCs eliminated the survival advantage of the

vaccinated *Nlrp3*$^{-/-}$ mice over WT mice (*HR = 1.15, p = 0.75*) (Fig. 5D). This change was exclusively due to an improvement in overall survival in the WT mice from 9.1% to 38.9% (*HR = 2.06, p <0.05*). There was no difference in overall survival of the vaccinated *Nlrp3*$^{-/-}$ mice after MDSC depletion (*40.0% vs. 35.0%, p = 0.82*). As a control, we measured survival in unvaccinated WT and -*Nlrp3*$^{-/-}$ following MDSC depletion. Survival was not significantly different from unvaccinated mice without MDSC depletion (Supplementary Fig. S6). Together, these results strongly suggested the decreased number of tumor-associated MDSCs accounted for the increased efficacy of the DC vaccine in *Nlrp3*$^{-/-}$ mice.

Nlrp3 expression promotes migration of MDSCs into the tumor

We assessed the effect of Nlrp3 on migration by isolating splenic MDSCs from WT and *Nlrp3*$^{-/-}$ mice and then transferring those cells to *Nlrp3*$^{-/-}$ mice with subcutaneous tumors. A population of MDSCs with greater than 90% purity could be effectively isolated with proper titration of the Gr-1 antibody and immunomagnetic bead selection (Supplementary Fig. S7). Furthermore, there were no differences in percentages of the subpopulations between WT and *Nlrp3*$^{-/-}$ cells (Fig. 5E).

This approach revealed significantly fewer *Nlrp3*$^{-/-}$ MDSCs migrated into the tumor compared to WT MDSCs (*178.1 ± 91.0 cells/tumor vs. 448.0 ± 36.1 cells/tumor, p < 0.05*) (Fig. 5E). These results were not biased by tumor size since no difference in tumor size was detected at the time of injection (*4.1 ± 0.06 mm vs. 4.2 ± 0.25 mm. p = NS*).

Discussion

DC vaccines represent a promising therapy for cancer; however, their efficacy is frequently suboptimal. For example, a recent prostate cancer vaccine trial found treatment resulted in a superior outcome, but the improvement in median survival was only 4.1 months (33). The very modest efficacy of DC vaccination was substantiated in our model by the vaccine's inability to improve survival in WT mice. However, we found the efficacy of DC vaccination could be markedly improved in the absence of Nlrp3.

The effect of Nlrp3 in the tumor environment was unanticipated because the established signals for inflammasome priming and activation are not present. Our results and those of others suggest this concept is changing. Li *et al*. have shown the Nlrp3 inflammasome can be activated in a sterile setting by necrotic cancer cells (35). Priming is accomplished by an excess of extra-cellular matrix components and activation is completed by ATP released from dying cancer cells (36). These observations required either the administration of 1×10^7 pressurized cells (37) or chemotherapy (36). Our work extends these ideas to the activation of Nlrp3 in the DC vaccine setting.

Further analysis implicated differences in MDSC number as the reason for the survival advantage in vaccinated *Nlrp3*$^{-/-}$ mice. Nlrp3 does not appear to affect the ability of MDSCs to suppress T cells. Instead, the reduction in quantity of MDSCs resulted in an inhibition of cytotoxic $CD8^+$ T cells and prompted a more effective antitumor response.

Our interpretation also explains why the administration of anti-Gr-1 antibodies restored the efficacy of the vaccine in WT mice to a degree comparable with *Nlrp3*$^{-/-}$ mice. Antibody depletion of Gr-1^+ cells is well established in the literature (35,38–41) though the effect of this depletion has had mixed results in cancer models (43). Improvement in anti-tumor immunity has been documented in models using UV light-induced tumors (42), liver carcinoma (35) and 15–12RM sarcoma cells (39). Our paper also demonstrates improvement in WT mice and is the first to do so using a DC vaccine. On the other hand, injection with

the Gr-1 antibody inhibited the immune response to a colon cancer cell line (38) and a NK sensitive lymphoma (40). These differences reflect the functional heterogeneity of MDSCs that is in part due to the tumor model used (43).

Though WT MDSCs were 2.5 times more efficient in migrating to the tumor, we did not find differences in the number of MDSCs in the TDLN. This finding suggests MDSCs are mobilized to the lymph node independently of Nlrp3. We believe mobilization to the spleen is also Nlrp3 independent since lower number of splenic *Nlrp3*$^{-/-}$ MDSCs correlated with tumor size. This observation suggests a critically important role for Nlrp3 in the recruitment of MDSCs solely to the tumor microenvironment.

It is conceivable that the differences in the number of MDSCs present at the site of tumor growth are due to changes in proliferation or survival. We believe our explanation of a role for Nlrp3 in MDSC migration is more consistent with the literature. Nlrp3 is more likely to induce cell death than cell survival. This effect has been documented in monocytes (47). Furthermore, *Nlrp3*$^{-/-}$ myeloid cells are resistant to cell death induced by bacterial pathogens (28). Wild type MDSCs are also not likely to have a proliferative advantage over *Nlrp3*$^{-/-}$ cells. MDSC expansion appears to take place in niches distant from the tumor in the spleen, bone marrow, and liver (48,49). The modest difference in the number of MDSCs in the spleen is not compatible with the significantly different numbers of MDSCs at the tumor site and strongly argues against proliferation as the sole reason for differences in tumor-associated MDSC number.

Though the improvement in the response to the DC vaccine is encouraging, a majority of tumors continue to grow even in *Nlrp3*$^{-/-}$ vaccinated mice. This finding is not particularly surprising since there are no vaccine-only strategies that have consistently eliminated established B16 F10 tumors (50). Though other forms of immune escape may also be at work, we are particularly intrigued by the significant contribution of the Nlrp3 inflammasome, given the presence of Nlrp3 independent inflammasomes. For example, inflammasomes containing absent in melanoma 2 (AIM2) (51) and ice protease-activating factor (Ipaf), contribute to IL-1β production independent of Nlrp3. An even greater anti-tumor response might be seen with inhibition of apoptosis-associated speck-like protein containing a CARD (ASC) since ASC is common to multiple inflammasomes. Those studies are underway in our laboratory.

At first glance, our result stands in contrast to recent findings that Nlrp3 might enhance adaptive immunity. For example, Ghiringhelli et al. demonstrated the Nlrp3 inflammasome was critically important in the P2X7R-dependent activation of DCs to generate IFN-γ producing $CD8^+$ T cells (36). As previously mentioned, this was mediated by the release of ATP from dying tumor cells in the presence of the chemotherapeutic drugs. Besides the inclusion of chemotherapy, one significant difference in this study was the addition of IL-12, which bypasses the requirement for the Nlrp3 inflammasome. We have found IL-12 is significantly generated by the DCs used by our group. Therefore, our findings suggest that in the presence of IL-12, activation of the Nlrp3 inflammasome enhances the accumulation of MDSCs and suppresses immune responses.

In summary, the expression of Nlrp3 in the tumor microenvironment diminishes antitumor immunity and vaccine efficacy by facilitating the migration of MDSCs to the site of the tumor. Since MDSCs express Nlrp3, their influx becomes part of a positive feedback loop leading to further expansion of these cells. These findings suggest novel means of increasing the effectiveness of DC vaccines by targeting the Nlrp3 inflammasome.

Supplementary Material

Refer to Web version on PubMed Central for supplementary material.

Acknowledgments

Grant Support: UNC UCRF grant to JT and HVD, P50 CA058223 to JS. JB was supported by an immunology training grant (T32 AI072273).

References

1. Martinon F, Mayor A, Tschopp J. The Inflammasomes: Guardians of the body. Annu Rev Immunol. 2009; 27:229–265. [PubMed: 19302040]
2. Ting J, Lovering R, Alnemri E, et al. The NLR gene family: A standard nomenclature. Immunity. 2008; 28:285–287. [PubMed: 18341998]
3. Mariathasan S, Monack DM. Inflammasome adaptors and sensors: Intracellular regulators of infection and inflammation. Nat Rev Immunol. 2007; 7:31–40. [PubMed: 17186029]
4. Agostini L, Martinon F, Burns K, McDermott MF, Hawkins P, Tschopp J. NALP3 forms an IL-1beta-processing inflammasome with increased activity in Muckle-Wells autoinflammatory disorder. Immunity. 2004; 20:319–25. [PubMed: 15030775]
5. Kono H, Rock K. How dying cells alert the immune system to danger. Nat Rev Imm. 2008; 8:279–289.
6. Guo L, Wei G, Shu J, et al. IL-1 family members and STAT activators induce cytokine production by Th2, Th17, and Th1 cells. PNAS. 2009; 106:13463–13468. [PubMed: 19666510]
7. Shi Y, Zheng W, Rock K. Cell injury releases endogenous adjuvants that stimulate cytotoxic T cell responses. PNAS. 2000; 97:14590–14595. [PubMed: 11106387]
8. Schroder K, Zhou R, Tschopp J. The NLRP3 Inflammasome: A sensor for metabolic danger? Science. 2010; 1184003:296–300. [PubMed: 20075245]
9. Saijo Y, Tanaka M, Miki M, et al. Proinflammatory cytokine IL-1 beta promotes tumor growth of Lewis lung carcinoma by induction of angiogenic factors: In vivo analysis of tumor-stromal interaction. J Immunol. 2002; 169:469–75. [PubMed: 12077278]
10. Krelin Y, Voronov E, Dotan S, et al. Interleukin-1beta-driven inflammation promotes the development and invasiveness of chemical carcinogen-induced tumors. Cancer Res. 2007; 67:1062–71. [PubMed: 17283139]
11. Lavi G, Voronov E, Dinarello CA, Apte RN, Cohen S. Sustained delivery of IL-1Rα from biodegradable microspheres reduces the number of murine B16 melanoma lung metastases. J Control Release. 2007; 123:123–130. [PubMed: 17900737]
12. Voronov E, Shouval DS, Krelin Y, et al. IL-1 is required for tumor invasiveness and angiogenesis. PNAS. 2003; 100:2645–2650. [PubMed: 12598651]
13. El-Omar EM, Carrington M, Chow WH, McColl KL, Bream JH, et al. Interleukin-1 polymorphisms associated with increased risk of gastric cancer. Nature. 2000; 404:398–402. [PubMed: 10746728]
14. Nikiteas N, Yannopoulos A, Chatzitheofylaktou A, Tsigris C. Heterozygosity for interleukin-18 607 A/C polymorphism is associated with risk for colorectal cancer. Anticancer Res. 2007; 27:3849–53. [PubMed: 18225542]
15. Tangkijvanich P, Thong-Ngam D, Mahachai V, Theamboonlers A, Poovorawan Y. Role of serum interleukin-18 as a prognostic factor in patients with hepatocellular carcinoma. World J Gastroenterol. 2007; 13:4345–9. [PubMed: 17708609]
16. Tu S, Bhagat G, Cui G, et al. Overexpression of interleukin-1β induces gastric inflammation and cancer and mobilizes myeloid-derived suppressor cells in mice. Cancer Cell. 2008; 14:408–419. [PubMed: 18977329]
17. Lechner MG, Liebertz DJ, Epstein AL. Characterization of cytokine-induced myeloid-derived suppressor cells from normal human peripheral blood mononuclear cells. J Immunol. 2010; 185(4):2273–84. [PubMed: 20644162]

18. Gabrilovich D, Bronte V, Chen S, et al. The terminology issue for myeloid-derived suppressor cells. Cancer Res. 2007; 67:425–6. [PubMed: 17210725]
19. Talmadge J. Pathways mediating the expansion and immunosuppressive activity of myeloid-derived suppressor cells and their relevance to cancer therapy. Clin Cancer Res. 2007; 13:5243–5248. [PubMed: 17875751]
20. Huang B, Pan P, Li Q, et al. Gr-1+CD115+ immature myeloid suppressor cells mediate the development of tumor-induced T regulatory cells and T-cell anergy in tumor-bearing host. Cancer Res. 2006; 66:1123–1131. [PubMed: 16424049]
21. Sinha P, Clements V, Bunt S, Albelda S, Ostrand-Rosenberg S. Cross-talk between myeloid-derived suppressor cells and macrophages subverts tumor immunity toward a type 2 response. J Immunol. 2007; 179:977–83. [PubMed: 17617589]
22. Hoechst B, Voigtnaender T, Ormandy L, et al. Myeloid derived suppressor cells inhibit natural killer cells in patients with hepatocellular carcinoma via the NKp30 receptor. Hepatology. 2009; 50:799–807. [PubMed: 19551844]
23. Yang L, DeBusk LM, Fukuda K, et al. Expansion of myeloid immune suppressor Gr+CD11b+ cells in tumor-bearing host directly promotes tumor angiogenesis. Cancer Cell. 2004; 6:409–421. [PubMed: 15488763]
24. Diaz-Montero C, Salem ML, Nishimura MI, Garrett-Mayer E, Cole DJ, Montero AJ. Increased circulating myeloid-derived suppressor cells correlate with clinical cancer stage, metastatic tumor burden, and doxorubicin-cyclophosphamide chemotherapy. Cancer Immunol Immunother. 2009; 58:49–59. [PubMed: 18446337]
25. Young M, Lathers D. Myeloid progenitor cells mediate immune suppression in patients with head and neck cancers. Int Immunopharmacol. 1999; 21:241–252.
26. Zea A, Rodriguez PC, Atkins MB, et al. Arginase-producing myeloid suppressor cells in renal cell carcinoma patients: A mechanism of tumor evasion. Cancer Res. 2005; 65:3044–3048. [PubMed: 15833831]
27. Melani C, Chiodoni C, Forni G, Colombo M. Myeloid cell expansion elicited by the progression of spontaneous mammary carcinomas in c-erbB-2 transgenic BALB/c mice suppresses immune reactivity. Blood. 2003; 102:2138–2145. [PubMed: 12750171]
28. Willingham SB, Allen IC, Bergstralh DT, et al. NLRP3 (NALP3, Cryopyrin) facilitates in vivo caspase-1 activation, necrosis, and HMGB1 release via inflammasome-dependent and-independent pathways. J Immunol. 2009; 183:2008–2015. [PubMed: 19587006]
29. Moran T, Burgents JE, Long B, et al. Alphaviral vector-transduced dendritic cells are successful therapeutic vaccines against neu-overexpressing tumors in wild-type mice. Vaccine. 2007; 25:6604–6612. [PubMed: 17675184]
30. van Deventer H, Wu QP, Bergstralh DT, et al. C-C chemokine receptor 5 on pulmonary fibrocytes facilitates migration and promotes metastasis via matrix metalloproteinase 9. Am J Pathol. 2008; 173:253–64. [PubMed: 18535183]
31. Burgents JE, Moran TP, West ML, Davis NL, Johnston RE, Serody JS. The immunosuppressive tumor environment is the major impediment to successful therapeutic vaccination in Neu transgenic mice. J Immunother. 2010; 33:482–491. [PubMed: 20463599]
32. Youn J-I, Nagaraj S, Collazo M, Gabrilovich D. Subsets of myeloid-derived suppressor cells in tumor-bearing mice. J Immunol. 2008; 181:5791–5802. [PubMed: 18832739]
33. Kantoff PW, Higano CS, Shore ND, et al. Sipuleucel-T immunotherapy for castration-resistant prostate cancer. NEJM. 2010; 363:411–422. [PubMed: 20818862]
34. Ko JS, Rayman P, Ireland J, et al. Direct and differential suppression of myeloid-derived suppressor cell subsets by sunitinib is compartmentally constrained. Cancer Res. 2010; 70:3526–3536. [PubMed: 20406969]
35. Li H, Ambade A, Re F. Cutting Edge: Necrosis activates the NLRP3 inflammasome. J Immunol. 2009; 183:1528–1532. [PubMed: 19596994]
36. Ghiringhelli F, Apetoh L, Tesniere A, et al. Activation of the NLRP3 inflammasome in dendritic cells induces IL-1beta-dependent adaptive immunity against tumors. Nat Med. 2009; 10:1170–1178. [PubMed: 19767732]

37. Iyer S, Pulskens WP, Sadler JJ, et al. Necrotic cells trigger a sterile inflammatory response through the Nlrp3 inflammasome. PNAS. 2009; 106:20388–20393. [PubMed: 19918053]
38. Stoppacciaro A, Melani C, Parenza M, et al. Regression of an established tumor genetically modified to release granulocyte colony-stimulating factor requires granulocyte-T cell cooperation and T cell-produced interferon gamma. J Exp Med. 1993; 178:151–161. [PubMed: 7686211]
39. Terabe M, Matsui S, Park JM, et al. Transforming growth factor-{beta} production and myeloid cells are an effector mechanism through which CD1d-restricted T cells block cytotoxic T lymphocyte-mediated tumor immunosurveillance: Abrogation prevents tumor recurrence. J Exp Med. 2003; 198:1741–1752. [PubMed: 14657224]
40. Nausch N, Galani IE, Schlecker E, Cerwenka A. Mononuclear myeloid-derived “suppressor” cells express RAE-1 and activate natural killer cells. Blood. 2008; 112:4080–4089. [PubMed: 18753637]
41. Matsuzaki J, Tsuji T, Chamoto K, Takeshima T, Sendo F, Nishimura T. Successful elimination of memory-type CD8+ T cell subsets by the administration of anti-Gr-1 monoclonal antibody in vivo. Cell Immunol. 2003; 224:98–105. [PubMed: 14609575]
42. Seung LP, Rowley DA, Dubey P, Schreiber H. Synergy between T-cell immunity and inhibition of paracrine stimulation causes tumor rejection. Proc Natl Acad Sci. 1995; 92:6254–6248. [PubMed: 7603979]
43. Dolcetti L, Peranzoni E, Ugel S, et al. Hierarchy of immunosuppressive strength among myeloid-derived suppressor cell subsets is determined by GM-CSF. Eur J Immunol. 2009; 40:22–35. [PubMed: 19941314]
44. Kool M, Petrilli V, DeSmedt T, et al. Cutting edge: Alum adjuvant stimulates inflammatory dendritic cells through the activation of the NALP3 inflammasome. J Immunol. 2008; 181:3755–9. [PubMed: 18768827]
45. Bjorkdahl O, Wingren A, Hedhund G, Ohlsson L, Dohlsten M. Vaccination with B16 melanoma cells expressing a secreted form of interleukin-1β induces tumor growth inhibition and an enhanced immunity against the wild-type B16 tumor. Cancer Immunol Immunother. 1997; 44:273–81. [PubMed: 9247562]
46. Bunt S, Yang L, Sinha P, Clements VK, Leips J, Ostrand-Rosenberg S. Reduced inflammation in the tumor microenvironment delays the accumulation of myeloid-derived suppressor cells and limits tumor progression. Cancer Res. 2007; 67:10019–10026. [PubMed: 17942936]
47. Fujisawa A, Kambe N, Saito M, et al. Disease-associated mutations in CIAS1 induce cathepsin B-dependent rapid cell death of human THP-1 monocytic cells. Blood. 2007; 109:2903–11. [PubMed: 17164343]
48. Liu C, Yu S, Kappes J, et al. Expansion of spleen myeloid suppressor cells represses NK cell cytotoxicity in tumor-bearing host. Blood. 2007; 109:4336–42. [PubMed: 17244679]
49. Ilkovitch D, Lopez D. The liver is a site for tumor-induced myeloid-derived suppressor cell accumulation and immunosuppression. Cancer Res. 2009; 69:5514–5521. [PubMed: 19549903]
50. Kochenderfer JN, Gress RE. A comparison and critical analysis of preclinical anticancer vaccination strategies. Exp Biol Med (Maywood). 2007; 232:1130–1141. [PubMed: 17895521]
51. Hornung V, Ablasser A, Charrel-Dennis M, et al. AIM2 recognizes cytosolic dsDNA and forms a caspase-1-activating inflammasome with ASC. Nature. 2009; 458:514–518. [PubMed: 19158675]

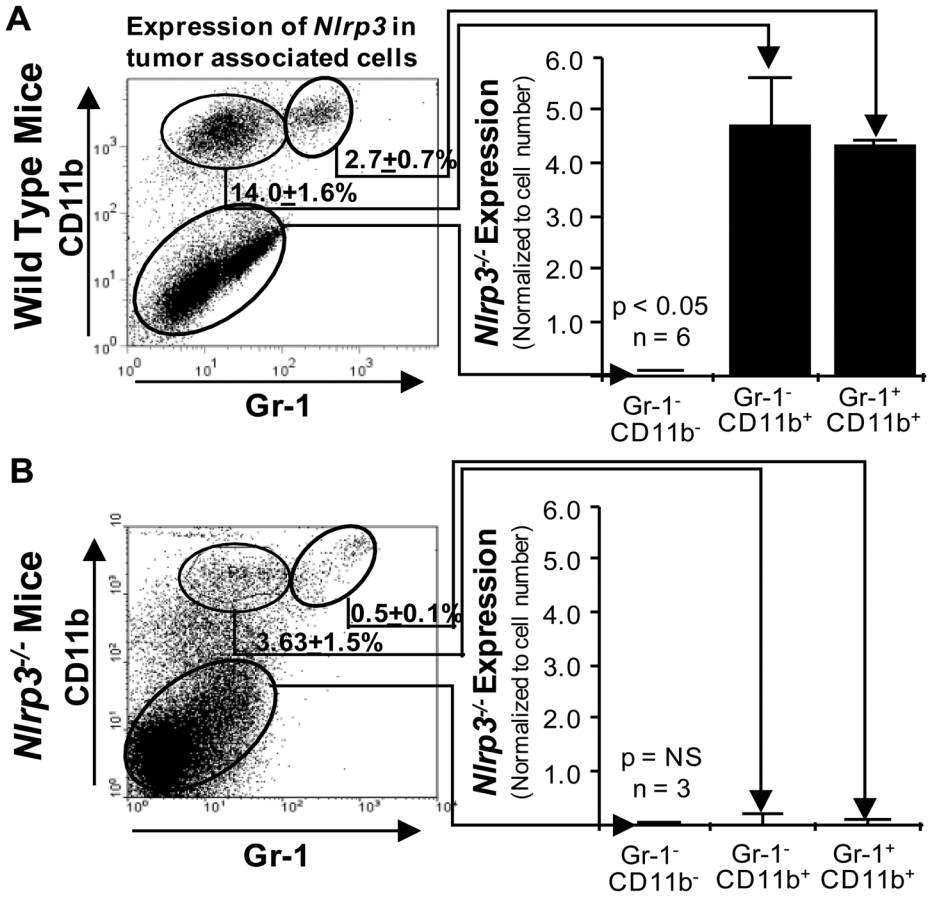

Figure 1. Nlrp3 is expressed by tumor-associated myeloid cells

Expression of *Nlrp3* by real time PCR in (1) Gr-1$^+$, CD11b$^+$ (2) Gr-1$^-$, CD11b$^+$ and (3) Gr-1$^-$, CD11b$^-$ sorted cells. The panel on left is a representative dot plot of sorted cells from a subcutaneous B16-F10 tumor in a vaccinated WT (A) and *Nlrp3*$^{-/-}$ mouse (B). The panel on the right is a bar graph of *Nlrp3* transcripts normalized to cell number.

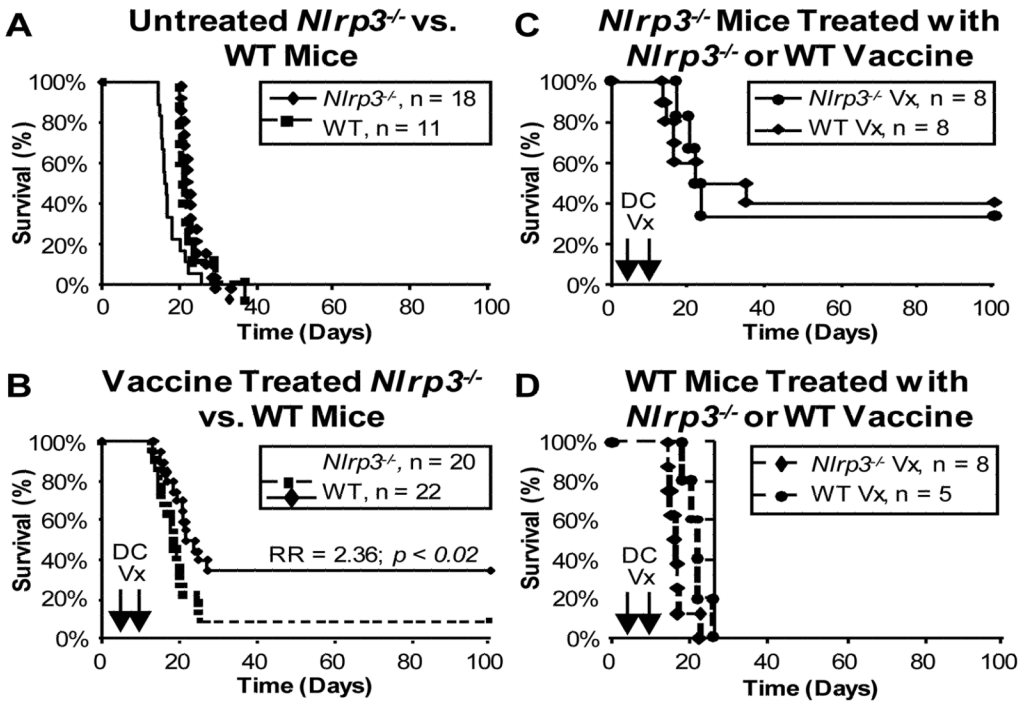

Figure 2. DC vaccine improves survival in Nlrp3$^{-/-}$ mice but not WT mice

(A) Survival curves of WT and *Nlrp3*$^{-/-}$ mice after receiving a subcutaneous injection with 1×10^4 B16-F10 melanoma cells. (B) Survival of *Nlrp3*$^{-/-}$ mice was significantly improved after receiving 1×10^6 tumor-lysate pulsed DCs (DC Vx) on day 3 and 10 after tumor injection. No improvement was seen in WT mice. (C) *Nlrp3*$^{-/-}$ mice show improved survival after receiving vaccines from either *Nlrp3*$^{-/-}$ or WT mice. (D) WT mice show no improvement in survival after receiving vaccines from WT or *Nlrp3*$^{-/-}$ mice.

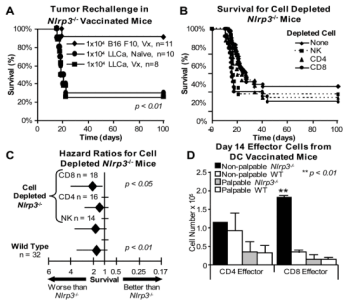

Figure 3. Vaccinated Nlrp3$^{-/-}$ mice demonstrate greater CD8^{+} T cell response

(A) Survival curves of vaccinated (Vx) or naive *Nlrp3*$^{-/-}$ mice after rechallenge with B16-F10 or Lewis Lung cancer (LLCa) cells. (B) Survival of vaccinated *Nlrp3*$^{-/-}$ mice following depletion of CD8^{+}, CD4^{+}, and NK cells. (C) The graph shows the hazard ratio and confidence intervals that compare survival of cell depleted *Nlrp3*$^{-/-}$ with control *Nlrp3*$^{-/-}$ mice. Values greater than 1 (to the left) demonstrate decreased survival compared to untreated *Nlrp3*$^{-/-}$ mice. (D) Total number of CD4^{+} and CD8^{+} effector cells from DC vaccinated *Nlrp3*$^{-/-}$ (black) and WT (gray) mice. Palpable tumors (gray) were defined by a measurable difference (> 0.2 mm) between the right and left leg; non-palpable tumors were grossly identifiable during dissection.

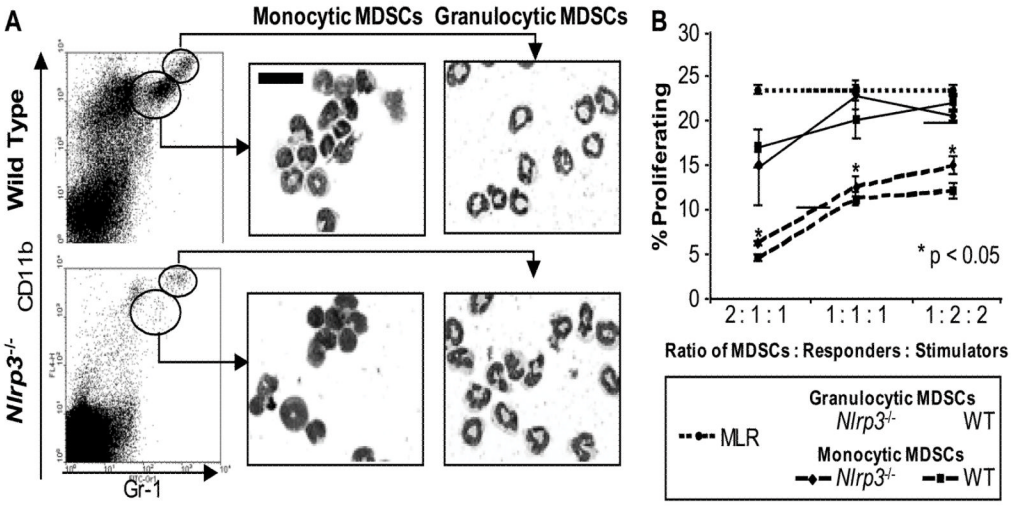

Figure 4. WT and Nlrp3$^{-/-}$ MDSCs have a similar microscopic appearance and suppressive capacity

(A) Flow cytometry dot plots for tumor-associated cells isolated from vaccinated WT and *Nlrp3*$^{-/-}$ mice. Cells were sorted by the gates shown and then examined after cytospin with Wright Giemsa staining. Lens magnification is 500X; scale bar is 20 μm. (B) Line graph showing suppression of a MLR reaction by granulocytic (solid line) and monocytic (dashed line) MDSCs from WT (squares) and *Nlrp3*$^{-/-}$ (diamonds) mice. Significance was determined by comparing proliferation with control MLR response (dotted line). Results are averaged from three separate experiments.

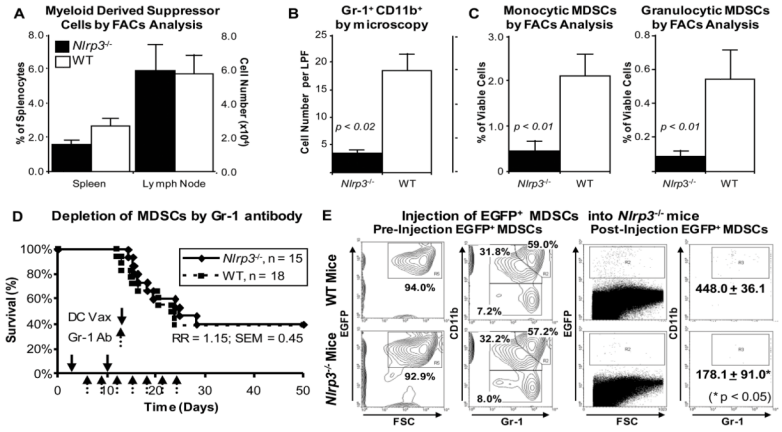

Figure 5. Superior response to DC vaccines by Nlrp3$^{-/-}$ mice is due to impaired migration of MDSCs

(A) Percentages of MDSCs from the spleen and total number of MDSCs in the TDLN of WT (striped) and *Nlrp3*$^{-/-}$ (solid) mice as determined by flow cytometry 14 days after tumor injection. (B) The total number of tumor-associated Gr-1^{+}, CD11b^{+} cells is increased in WT mice as determined by microscopy. (C) Increased percentage of monocytic MDSCs (left) and granulocytic MDSCs (right) from the tumor of WT (striped) compared to *Nlrp3*$^{-/-}$ (solid) mice as determined by flow cytometry. (D) Survival curves of WT and *Nlrp3*$^{-/-}$ mice treated with anti-Gr-1 antibody (dotted arrows) and DC vaccine (solid arrows). (E) Contour plots on the left show phenotype of MDSCs isolated from the spleens of WT (upper) and *Nlrp3*$^{-/-}$ (lower) mice prior to injection into *Nlrp3*$^{-/-}$ mice. Dot plots on the right show cells recovered from B16 tumors in vaccinated *Nlrp3*$^{-/-}$ mice. Upper panels are WT EGFP^{+} MDSCs and lower panels are *Nlrp3*$^{-/-}$ EGFP^{+} MDSCs. Values represent the average number of cells recovered from each tumor.